

## Pressure and nonlinear susceptibilities in QCD at finite chemical potentials

Rajiv V. Gavai\* and Sourendu Gupta†

*Department of Theoretical Physics, Tata Institute of Fundamental Research, Homi Bhabha Road, Mumbai 400005, India*

(Received 20 March 2003; published 25 August 2003)

When the free energy density of QCD is expanded in a Taylor series in the chemical potential  $\mu$ , the coefficients are the nonlinear quark number susceptibilities. We show that these depend on the prescription for putting the chemical potential on the lattice, making all extrapolations in the chemical potential prescription dependent at finite lattice spacing. To put bounds on the prescription dependence, we investigate the magnitude of the nonlinear susceptibilities over a range of temperature,  $T$ , in QCD with two degenerate flavors of light dynamical quarks at lattice spacing  $1/4T$ . The prescription dependence is removed in quenched QCD through a continuum extrapolation, and the dependence of the pressure  $P$  on  $\mu$  is obtained.

DOI: 10.1103/PhysRevD.68.034506

PACS number(s): 11.15.Ha, 12.38.Gc

One of the most important objects in the study of hot and dense hadronic matter is the phase diagram, particularly, the location of the critical end point, characterized by the temperature  $T_E$  and the chemical potential  $\mu_E$ . Much effort has been expended recently on estimating these quantities at finite lattice spacing,  $a$ , using, implicitly [1] or explicitly [2–4], a Taylor series expansion of the free energy density. This needs the nonlinear susceptibilities which define the response to an applied  $\mu$  beyond quadratic order. An equally important question for phenomenology arises from the fact that present day heavy-ion collision experiments access the part of the QCD phase diagram with  $\mu \approx 10\text{--}80$  MeV, i.e., baryon chemical potential  $\mu_B \approx 30\text{--}250$  MeV [5], far from  $\mu_E$ . It is then pertinent to ask how relevant the  $\mu=0$  lattice QCD computations of quantities such as the pressure  $P$  are to these experiments.

In this paper we present the first investigation of these nonlinear susceptibilities. We uncover essential lattice artifacts, but manage to quantify and remove them in the process of taking the continuum limit. We explicitly construct a Taylor series expansion for  $P$  at  $\mu > 0$ , put limits on the region of linear response, i.e., of reliable extrapolations, and show that the  $\mu=0$  lattice computations are clearly relevant to experiments. An interesting sidelight is that there is strong evidence of short thermalization times in the dense matter formed in these heavy-ion collisions [6], which may be related to large values of transport coefficients [7]. Most computations of such dynamical quantities are based on linear response theory. The success of the linear approximation in static quantities at fairly large driving also gives us confidence in using linear response theory for dynamics. Another interesting point is that the radius of convergence of a Taylor series expansion started near  $T_c$  [8] must give information on the location of the critical end point,  $(T_E, \mu_E)$ , through the Taylor coefficients, i.e., the nonlinear susceptibilities. Since these Taylor coefficients turn out to be prescription dependent and subject to strong finite lattice spacing effects, it seems that present day estimates of the end point will have to be sharpened strongly before they can be used as a guide to phenomenology.

The partition function of QCD at finite temperature  $T$  and chemical potentials  $\mu_f$  for each flavor  $f$  can be written as

$$Z \equiv e^{-F/T} = \int \mathcal{D}U e^{-S(T)} \prod_f \text{Det } M(m_f, T, \mu_f). \quad (1)$$

$F$  is the free energy,  $S$  is the gluon part of the action,  $M$  is the Dirac operator, each determinant is for one quark flavor and the temperature  $T$  enters through the shape of the lattice and boundary conditions [9]. We shall work with a lattice discretization and use staggered quarks [10]. In this work we shall only consider two degenerate flavors of quarks:  $m_u = m_d = m$  [11], with chemical potentials  $\mu_u$  and  $\mu_d$ . The number densities,  $n_f$ , and the (linear) quark number susceptibilities,  $\chi_{fg}$ , are the first and second derivatives of  $-F/V$  with respect to  $\mu_f$  and  $\mu_g$  [12]. Since  $P = -F/V$  for a homogeneous system, the nonlinear susceptibilities of order  $n \geq 3$  are also the remaining Taylor coefficients of an expansion of  $P$ ,

$$\chi_{fg\dots} = -\frac{1}{V} \frac{\partial^n F}{\partial \mu_f \partial \mu_g \dots} = \frac{T}{V} \frac{\partial^n \log Z}{\partial \mu_f \partial \mu_g \dots}, \quad (2)$$

where we construct the expansion around  $\mu_f = 0$ .

We now write systematic rules for the construction of the nonlinear susceptibilities. The derivatives of  $\log Z$  needed in Eq. (2) can be related to the derivatives of  $Z$  with respect to the chemical potentials  $\mu_f$ ,  $\mu_g$ , etc. (which we denote by  $Z_{fg\dots}$ ) by the usual formulas for taking connected parts [13]. The only extra point to remember is that all the odd derivatives vanish by  $CP$  symmetry. To write the subsequent formulas compactly, we define operators  $O_i$  by

$$Z_f = Z \langle O_1 \rangle, \quad \text{and} \quad O_{n+1} = \frac{\partial O_n}{\partial \mu_f}, \quad (3)$$

where angular brackets denote averages over the ensemble defined by Eq. (1) at  $\mu_f = 0$ . Diagrammatic rules [14] for the  $O_i$  and the derivatives of  $Z$ , are:

- (1) Put down  $n$  vertices (each corresponding to a derivative of  $M$  with respect to  $\mu_f$ ) and label each with its flavor index.

\*Electronic address: gavai@tifr.res.in

†Electronic address: sgupta@tifr.res.in

- (2) Join the vertices by lines (each representing a quark) into sets of closed loops such that each loop contains only vertices of a single flavor.  $O_i$  is denoted by a single loop joining  $i$  vertices.
- (3) For degenerate flavors and  $\mu_f=0$ , the operators are labeled only by the topology, which is specified completely by the number of vertices per loop and the number of such loops. Therefore erase the flavor index after step 2. We denote each resulting operator by the notation  $O_{ij\dots} = O_i O_j \dots$ , where  $i+j+\dots = n$ .
- (4) For each  $n$ th order derivative of  $Z$ , add all the operator topologies for fixed  $n$  with flavor-dependent multiplicity equal to the number of ways in which each topology arises given the flavor indices.

The number densities  $n_u = n_d = (T/V)\langle O_1 \rangle$  vanish at  $\mu=0$ . We have considered the (linear) susceptibilities  $\chi_3 = (T/V)\langle O_2 \rangle$  and  $\chi_{ud} = (T/V)\langle O_{11} \rangle$  extensively in a recent series of papers [21]. The new quantities that we now consider are the two third order derivatives

$$Z_{uuu} = Z\langle O_3 + 3O_{12} + O_{111} \rangle \quad \text{and} \quad Z_{uud} = Z\langle O_{12} + O_{111} \rangle, \quad (4)$$

the three fourth order derivatives

$$\begin{aligned} Z_{uuuu} &= Z\langle O_4 + 4O_{13} + 3O_{22} + 6O_{112} + O_{1111} \rangle, \\ Z_{uuud} &= Z\langle O_{13} + 3O_{112} + O_{1111} \rangle, \\ Z_{uudd} &= Z\langle O_{22} + 2O_{112} + O_{1111} \rangle, \end{aligned} \quad (5)$$

and the five corresponding susceptibilities. The third order susceptibilities turn out to vanish. The fourth order susceptibilities are

$$\begin{aligned} \chi_{uuuu} &= \left( \frac{T}{V} \right) \left[ \frac{Z_{uuuu}}{Z} - 3 \left( \frac{Z_{uu}}{Z} \right)^2 \right], \\ \chi_{uuud} &= \left( \frac{T}{V} \right) \left[ \frac{Z_{uuud}}{Z} - 3 \left( \frac{Z_{uu}}{Z} \right) \left( \frac{Z_{ud}}{Z} \right) \right], \\ \chi_{uudd} &= \left( \frac{T}{V} \right) \left[ \frac{Z_{uudd}}{Z} - \left( \frac{Z_{uu}}{Z} \right)^2 - 2 \left( \frac{Z_{ud}}{Z} \right)^2 \right]. \end{aligned} \quad (6)$$

The operators contributing to Eqs. (4),(5) are shown in Fig. 1. Note the interesting fact that beyond the second order, the number of distinct operator topologies is greater than the number of susceptibilities [14]; however, by making  $N_f$  sufficiently large, all topologies up to any given order can be given a physical meaning.

A perturbative expansion in the continuum proceeds through an order-by-order enumeration of interaction terms. In the continuum the diagrams in Fig. 1 are the leading order (ideal quark gas) part of the perturbative expansion of the susceptibilities, where each vertex corresponds to the insertion of a  $\gamma_0$  (since the chemical potential enters the Lagrang-

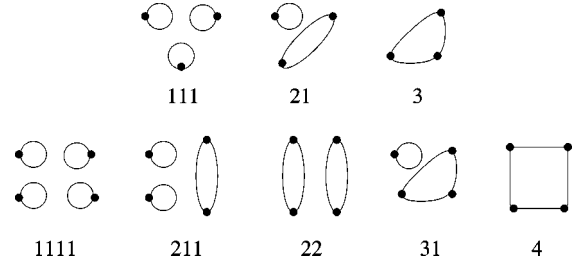


FIG. 1. All topologies which contribute to derivatives up to fourth order, and the notation for the corresponding operators.

ian as  $\gamma_0 \mu_f$ ). Higher order Feynman diagrams correspond to dressing these loops by gluon attachments in all possible ways.

In the lattice theory the diagrams in Fig. 1 stand for operator definitions which need further specification. They are not Feynman diagrams, but mnemonics for the process of taking derivatives of  $Z$ . Since the coupling of fermions to the chemical potential is nonlinear [15], hence all derivatives of  $M$  exist and are nonzero in general. Using the identity  $\text{Det } M = \exp(\text{Tr} \ln M)$  it is easy to get the usual expression  $O_1 = \text{Tr } M^{-1} M'$ , where  $M'$  is the first derivative of  $M$  with respect to a chemical potential. Next, using the chain rule

$$\frac{dM^{-1}}{d\mu_f} = -M^{-1} M' M^{-1}, \quad (7)$$

which comes from the identity  $MM^{-1}=1$ , we recover the relation  $O_2 = \text{Tr}[-M^{-1} M' M^{-1} M' + M^{-1} M'']$ , where  $M''$  is the second derivative of  $M$  with respect to the chemical potential. Higher operators can be derived by repeated application of the chain rule with Eq. (7), and involve higher derivatives of  $M$ , which we write as  $M^{(n)}$  (a systematic method for doing this is given in the Appendix). In particular,

$$\begin{aligned} O_3 &= \text{Tr}[2(M^{-1} M')^3 - 3M^{-1} M'' M^{-1} M' + M^{-1} M^{(3)}] \\ O_4 &= \text{Tr}[-6(M^{-1} M')^4 - 3(M^{-1} M'')^2 \\ &\quad + 12M^{-1} M'' (M^{-1} M')^2 - 4M^{-1} M^{(3)} M^{-1} M' \\ &\quad + M^{-1} M^{(4)}]. \end{aligned} \quad (8)$$

This completes the lattice definitions of the operators.

Before we proceed to evaluate them and extract the nonlinear susceptibilities, we note an ambiguity that arises on the lattice due to the fact that there is no unique way of putting chemical potential on the lattice. One can associate a factor  $f(a\mu)$  for the propagation of a quark forward in time by one lattice spacing and a factor  $g(a\mu)$  for the propagation of an antiquark. There are exactly four physical conditions that these two functions must satisfy [15]. In the absence of chemical potential the usual lattice theory must be recovered, hence  $f(0)=g(0)=1$ .  $CP$  symmetry gives  $f(-a\mu)=g(a\mu)$ . Finiteness of the energy density is guaranteed if  $f(a\mu)g(a\mu)=1$ . Finally, the correct continuum limit requires  $f'(0)=1$ . These constraints imply the further relations,  $f''(0)=1$  and  $f^{(n)}(0)=(-1)^n g^{(n)}(0)$ , where the su-

perscript  $n$  on  $f$  and  $g$  denotes the  $n$ th derivative. All this guarantees that  $n_f$  and  $\chi_{fg}$  are prescription independent.

The four conditions above also give relations between the remaining  $f^{(n)}$ , such as  $f^{(4)}=4f^{(3)}-3$ , but do not fix their numerical values. Since  $\mu$  appears linearly in the continuum Lagrangian, these higher derivatives are all lattice artifacts. Any extra conditions imposed to fix them cannot be physical, and must remain at the level of prescription. The usual prescription,  $f(a\mu)=\exp(a\mu)$  [16], which we call the HK prescription, gives  $f^{(n)}(0)=1$ , but the alternative BG prescription  $f(a\mu)=(1+a\mu)/\sqrt{(1-a^2\mu^2)}$  [17] gives  $f^{(3)}(0)=3$  and  $f^{(4)}(0)=9$ .

The difference between the two prescriptions can be rather significant. At any fixed cutoff, one may try to roughly map two prescriptions on to each other by changing  $\mu$  while holding  $Z$  fixed by keeping  $f(a\mu)$  unchanged. This gives the relation that for constant physics we must have

$$a\mu_{BG}=\tanh(a\mu_{HK}), \quad (9)$$

where this mapping is for quark chemical potentials. On  $N_t=4$  lattices, the critical end point for 2+1 flavor QCD has been determined to be at  $T_E=160\pm 3.5$  MeV and  $\mu_E^{HK}=725\pm 35$  MeV [1]. The matching formula of Eq. (9) then shows that  $\mu_E^{BG}\simeq 692$  MeV, and hence the resultant uncertainty in  $\mu_E$  from this source alone is comparable to the statistical errors. We next show that this ambiguity vanishes in the continuum limit in all prescriptions. We also show later (Table II) that uncertainties of almost 20% are also expected from other finite lattice spacing effects even within one prescription, and lattice spacings of  $1/12T_E$  may be required to find  $\mu_E$  stable within statistical error bars.

This freedom of choosing a prescription has specific consequences for the third and higher derivatives of  $M$ , and through them for the nonlinear susceptibilities, and hence for  $F$ ,  $P$  and all quantities at finite  $\mu$  and  $a$ . At  $\mu_f=0$ , the derivatives of  $M$  are related by

$$\begin{aligned} M^{(n)} &= f^{(n)} a^{n-2} M' \quad (n \text{ odd}), \\ M^{(n)} &= f^{(n)} a^{n-2} M'' \quad (n \text{ even}). \end{aligned} \quad (10)$$

As a result,  $O_3=O_3^{HK}+\Delta f^{(3)}a^2O_1$  and  $O_4=O_4^{HK}+4\Delta f^{(3)}a^2O_2$ , where the superscript HK on an operator denotes its value obtained in the HK prescription and  $\Delta f^{(3)}=f^{(3)}-1$ . Clearly, the prescription dependence, manifested as a nonvanishing  $\Delta f^{(3)}$  at this order, disappears in the continuum limit,  $a\rightarrow 0$ . Since  $\langle O_1 \rangle=0$  at  $\mu=0$ , the prescription dependence of  $\langle O_3 \rangle$  is invisible. We find that  $\chi_{uuud}=\chi_{uuud}^{HK}+\Delta f^{(3)}(\chi_{ud}/T^2)/N_t^2$ . Since  $\chi_{ud}$  vanishes within errors, as we show later,  $\chi_{uuud}$  turns out to be effectively prescription independent. From the relation for  $O_4$  we find, on varying  $N_t$  at fixed  $T$ ,

$$\chi_{uuuu}=\chi_{uuuu}^{HK}+\Delta f^{(3)}\left(\frac{\chi_{uu}}{T^2}\right)\left(\frac{4}{N_t^2}\right). \quad (11)$$

Finally,  $\chi_{uudd}$  involves neither  $M^{(3)}$  nor  $M^{(4)}$ , and hence is prescription independent. The prescription dependence of

TABLE I. Results in two flavor QCD with sea quark  $m/T_c=0.1$ . For  $T=T_c$  the results are based on 2017 configurations, for  $1.5T_c$  on 370, for  $2T_c$  on 126 and for  $3T_c$  on 60. At  $T_c$  and  $3T_c$  100 noise vectors were used.  $\chi_{uuuu}$  can be extracted from  $\mu_*$  and  $\chi_{uu}$  using Eq. (13).

$T/T_c$	$m_V/T$	$10^6\chi_{ud}/T^2$	$10^6\chi_{uuud}$	$10^4\chi_{uudd}$	$\mu_*^{HK}/T$
1.0	0.2	-15 (5)	3 (1)	7 (1)	3.20 (3)
	0.1	-8 (3)	6 (3)	9 (2)	3.31 (5)
	0.03	-19 (14)	3 (19)	11 (2)	3.38 (4)
1.5	0.2	-0.3 (22)	-0.7 (6)	0.107 (3)	3.73 (1)
	0.1	0.6 (22)	-0.6 (7)	0.105 (3)	3.84 (1)
	0.03	-0.07 (22)	-0.5 (9)	0.106 (3)	3.86 (2)
2.0	0.2	2 (3)	0.5 (7)	0.097 (3)	3.83 (1)
	0.1	2 (3)	0.5 (7)	0.098 (3)	3.87 (1)
	0.03	1 (3)	0.6 (7)	0.096 (3)	3.78 (2)
3.0	0.2	0.6 (3)	0.12 (8)	0.032 (2)	3.87 (1)
	0.1	0.6 (3)	0.12 (8)	0.033 (2)	3.88 (2)
	0.03	0.6 (3)	0.12 (8)	0.033 (2)	3.88 (2)

other susceptibilities can be systematically worked out, and it can be shown exactly as above that they become physical only in the continuum. Mixed derivatives of  $T$  and  $\mu$  also have similar behavior. If the dependence on  $a$  of each susceptibility were known in any scheme, then one could write down an improved prescription by removing finite  $a$  effects systematically. In other schemes every quantity is potentially prescription dependent at finite lattice spacing.

After this analysis of lattice artifacts in the Taylor coefficients, we return to the Taylor expansion itself. Along the line  $\mu_u=\mu_d=\mu$ , the Taylor series expansion of  $P$  can be written in the form

$$\frac{\Delta P}{T^4}=\left(\frac{\chi_{uu}}{T^2}\right)\left(\frac{\mu}{T}\right)^2\left[1+\left(\frac{\mu/T}{\mu_*/T}\right)^2+O\left(\frac{\mu^4}{\mu_*^4}\right)\right], \quad (12)$$

where  $\Delta P=P(\mu)-P(\mu=0)$ , we have neglected  $\chi_{uudd}$  in anticipation of our numerical results (Tables I and II), and

$$\frac{\mu_*}{T}=\sqrt{\frac{12\chi_{uu}/T^2}{|\chi_{uuuu}|}}. \quad (13)$$

For an ideal gas in the continuum,  $\chi_{uu}/T^2=1$  and  $\chi_{uuuu}=6/\pi^2$ , giving  $\mu_*/T=\sqrt{2}\pi\simeq 4.43$ . Some remarks are in order.

- (1) The series within square brackets in Eq. (12) is prescription dependent at any nonzero lattice spacing, and hence physical values of  $\Delta P$  can be most reliably extracted by extrapolating each term in the series to the continuum.
- (2) For those values of  $\mu$  at which the second or higher order terms in the brackets in Eq. (12) are important, computations of  $\Delta P/T^4$  on lattices with finite  $N_t$  are necessarily prescription dependent. Since  $F=-PV$ , the same is evidently true for all other physical quantities,

TABLE II. Results in quenched QCD with  $m_v/T_c=0.1$ . Quadratic extrapolations to the continuum limit,  $N_t=\infty$ , from the last three points, are shown.  $\mu_*$  and  $\chi_{uuuu}$  are related by Eq. (13).

$T/T_c$	$N_t$	$10^6\chi_{ud}/T^2$	$10^6\chi_{uuud}$	$\chi_{uuuu}$	$\mu_*^{HK}/T$
1.5	4	2 (4)	-0.7 (8)	1.48 (2)	3.81 (2)
	8	0.2 (20)	0.2 (2)	0.70 (1)	4.36 (4)
	10	-0.4 (7)	0.04 (6)	0.61 (2)	4.47 (4)
	12	-0.5 (6)	0.00 (3)	0.56 (1)	4.55 (4)
	14	-0.3 (5)	-0.04 (3)	0.53 (1)	4.56 (4)
$\infty$			0.45 (1)	4.67 (4)	
2.0	4	3 (2)	0.9 (7)	1.51 (1)	3.83 (1)
	6	0.2 (9)	0.2 (1)	1.01 (1)	4.11 (1)
	8	-0.3 (2)	0.1 (2)	0.74 (1)	4.32 (5)
	10	-0.3 (5)	-0.05 (4)	6.37 (3)	4.45 (3)
	12	-0.1 (4)	0.00 (3)	0.58 (1)	4.56 (3)
	14	-0.2 (6)	0.00 (3)	0.56 (1)	4.59 (4)
$\infty$			0.49 (3)	4.76 (4)	
3.0	4	2 (4)	0.8 (8)	1.54 (1)	3.85 (1)
	8	1.9 (7)	0.12 (6)	0.79 (2)	4.25 (5)
	10	-0.1 (4)	0.01 (4)	0.66 (1)	4.40 (3)
	12	-0.1 (3)	-0.02 (1)	0.61 (1)	4.48 (4)
	14	-0.2 (1)	0.06 (4)	0.58 (1)	4.51 (2)
$\infty$			0.496 (1)	4.62 (1)	

including the energy density. From Eqs. (11) and (13), it is clear that the prescription dependence of the quadratic term is  $(\mu_*/T)^2/3N_t^2$ . For  $N_t=4$  this can be as large as 33% (see Table II).

- (3) If the series in Eq. (12) is well behaved, i.e., sixth and higher order susceptibilities are not much larger than  $\chi_{uuuu}$ , then this expansion must be well approximated by the leading term for  $\mu \ll \mu_*$  in every prescription, and hence be effectively independent of prescription [18]. Other finite lattice spacing effects may still exist.
- (4) The series expansion must fail to converge in the vicinity of a phase transition; therefore estimates of  $(T_E, \mu_E)$  on finite lattices must be prescription dependent, as we have already estimated. Computation of the continuum limit of several terms in the double series for  $F(T, \mu)$  may allow us to use series extrapolation methods, such as Padé approximants or estimates of radius of convergence [19], to identify  $(T_E, \mu_E)$  in the continuum limit.

We turn now to our numerical simulations. For dynamical sea quark mass  $m/T_c=0.1$  we studied the higher order susceptibilities at  $T=T_c$  on a  $4 \times 10^3$  lattice,  $1.5T_c$  and  $2T_c$  on  $4 \times 12^3$  lattices, and  $3T_c$  on a  $4 \times 14^3$  lattice. All the simulations were performed using the hybrid R-algorithm [20] with molecular dynamics trajectories integrated over one unit of MD time using a leap-frog algorithm with time step of 0.01 units. At  $T_c$  autocorrelations of the Wilson line and the quark condensate were found to be between 150 and 250 trajectories. With over 2000 saved configurations separated by 10 trajectories each, this gave the equivalent of about 100 inde-

pendent configurations. For  $T > T_c$  the autocorrelations were all less than ten trajectories, and hence all the saved configurations can be considered statistically independent.

Quark number susceptibilities were evaluated in the HK prescription on stored configurations using valence quark masses  $m_v/T_c=0.2, 0.1,$  and  $0.03$ . The smallest valence quark mass is chosen such that the ratio of the ( $T=0$ ) rho and pion masses reaches its physical value of 0.2 at the lattice spacing  $a=1/4T_c$ . All quark-line disconnected diagrams of the kind needed for these measurements are evaluated using a straightforward extension of the stochastic method given for  $\chi_{ud}$  in [21] using 10 to 100 noise vectors per configuration [22]. Our results for the nonlinear susceptibilities which do not vanish by symmetry are shown in Table I. It is clear that of these only  $\chi_{uuud}$  and  $\chi_{uuuu}$  are nonzero with statistical significance. Comparing them to computations with sea quark mass  $m/T_c=0.2$  and various volumes, we concluded that they are free of sea quark mass and finite volume effects. Also note the stability in physical quantities as  $m_v/T_c$  decreases from 0.1 to 0.03.

With present day computer resources the continuum limit is hard to take in QCD with dynamical quarks. To investigate this limit we have evaluated the same quantities in quenched QCD for  $T \geq 1.5T_c$  where the difference in the order of transitions is immaterial [23]. The run parameters are exactly as in [21]. Our results are shown in Table II. These results show that there is over 20% movement in  $\mu_*$  when going from  $N_t=4$  to the continuum within a fixed prescription. Since  $\mu_*$  is an estimate of the radius of convergence of the Taylor expansion at the fourth order, it implies that the estimate of the end point,  $\mu_E$ , may shift upward by about 20% due to finite size effects even inside the HK scheme.  $\chi_{uuud}$  remains significantly nonzero on all the lattices, and there is some evidence that it becomes either zero or marginally negative in the continuum [24]. We shall present more detailed studies in the future. Finally, the results for  $N_t=4$  are very similar in the quenched and dynamical theories, leading us to believe that the continuum limits will also be close.

$\Delta P/T^4$  obtained in quenched QCD, using values of  $\chi_{uu}$  from [21] and  $\mu_*/T$  obtained here, are shown in Fig. 2. At RHIC it is seen that  $\mu/T_c=0.06 \ll 0.15$ , which implies that  $\Delta P/T^4$  is negligible. In terms of dimensionless variables, the results in quenched and dynamical QCD are not expected to differ by more than 5–10% [25]. For  $\mu/T_c \approx 0.45$ , relevant to SPS energies, the effects of  $\mu > 0$  are more significant, but can still be reliably extracted using only the leading term of Eq. (12). In this whole range of  $\mu/T_c$  the results of [25], including a correction for finite lattice spacing artifacts in the evaluation of  $\chi_{uu}$  at  $N_t=4$ , are the same as our continuum results, and both are dominated by the leading term of Eq. (12). Our computations show that for  $\mu \geq 2T_c$ , higher order terms become significant for the continuum limit. As a result, at these chemical potentials, reweighting on  $N_t=4$  lattices, even after correcting for finite  $a$  effects in  $\chi_{uu}$ , are quite different from the continuum values.

In conclusion, we have studied nonlinear susceptibilities and have shown that they are prescription dependent at finite lattice spacing. We have found the continuum limit of these quantities in quenched QCD, and thereby removed these ar-

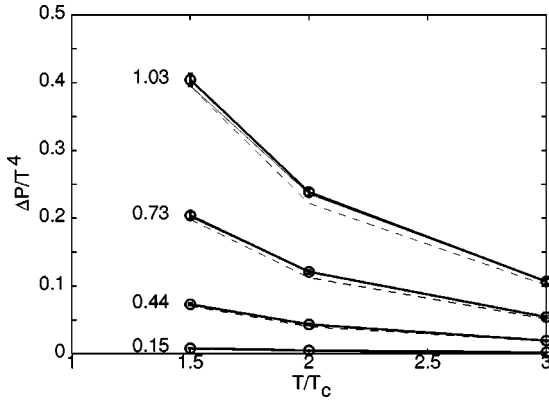


FIG. 2.  $\Delta P/T^4$  as a function of  $T/T_c$  for the values of  $\mu/T_c$  shown. Continuum results correct to  $O(\mu^4)$  (full lines) and  $O(\mu^2)$  (dotted lines) are shown.  $N_f=4$  results, in the HK prescription, correct to  $O(\mu^4)$  and multiplied by 0.47 to compensate for finite  $a$  effects in  $\chi_{uu}$  are shown with dashed lines.

tifacts. This allows us to compute the finite chemical potential corrections to the pressure relevant to RHIC and SPS experiments. For  $a=1/4T$  the numerical results for QCD with and without dynamical quarks are similar, and we find the continuum limit of some of these quantities in the quenched theory. It would be interesting to compare them with perturbation theory. We have argued that the lattice spacing ambiguity in the critical end point ( $T_E, \mu_E$ ) evaluated at  $N_f=4$  is significantly bigger than the statistical errors. As a result, a continuum extrapolation is required to obtain the physical value of the end point. This may be possible with the computation of several nonlinear susceptibilities.

We would like to thank J.-P. Blaizot for discussions.

#### APPENDIX: LATTICE OPERATORS

In this appendix we work in lattice units, i.e., we choose the lattice spacing to be unity. We introduce the compact notation

$$\begin{aligned} \text{Tr}[(M^{-1}M^{(p_1)})^{n_1}(M^{-1}M^{(p_2)})^{n_2}\dots] \\ = (n_1 \cdot p_1 \oplus n_2 \cdot p_2 \oplus \dots), \end{aligned} \quad (\text{A1})$$

and further write  $(1 \cdot p)$  as  $(p)$ . Since the trace allows only cyclic permutations, therefore

$$(a \oplus b \oplus c) = (c \oplus a \oplus b) \neq (b \oplus a \oplus c), \quad (\text{A2})$$

i.e., the ‘‘addition’’ (represented by  $\oplus$ ) is not commutative. ‘‘Multiplication’’ (denoted by the dot) is distributive over addition, subject to restrictions due to noncommutativity, i.e.,

$$(n \cdot p \oplus m \cdot p) = [(n+m) \cdot p],$$

$$(n \cdot p \oplus m \cdot p' \oplus l \cdot p) = [(n+l) \cdot p \oplus m \cdot p'], \quad (\text{A3})$$

but no simplification is possible for  $(n \cdot p \oplus m \cdot p' \oplus l \cdot p \oplus \dots)$ . Traces can be added, i.e.,

$$a(n \cdot p) + b(n \cdot p) = (a+b)(n \cdot p). \quad (\text{A4})$$

The point of all this is to simplify the taking of derivatives. These are easy to write,

$$(n \cdot p)' = -n(1 \oplus n \cdot p) + n[(n-1) \cdot p \oplus (p+1)]. \quad (\text{A5})$$

The operation of taking derivatives is linear over the ‘‘addition’’  $\oplus$ , since this is just the rule for taking derivatives of products.

We have the first examples,

$$O_1 = (1), \quad O_2 = -(2 \cdot 1) + (2). \quad (\text{A6})$$

Then, the remaining known ones are obtained simply by applying the rules again. Since  $(2 \cdot 1)' = -2(3 \cdot 1) + 2(1 \oplus 2)$  and  $(2)' = -(1 \oplus 2) + (3)$ , we first obtain the relation in Eq. (8),

$$O_3 = 2(3 \cdot 1) - 3(1 \oplus 2) + (3). \quad (\text{A7})$$

At the fourth order we need the derivatives

$$(3 \cdot 1)' = -3(4 \cdot 1) + 3(2 \cdot 1 \oplus 2),$$

$$(1 \oplus 2)' = -2(2 \cdot 1 \oplus 2) + (2 \cdot 2) + (1 \oplus 3),$$

$$(3)' = -(1 \oplus 3) + (4). \quad (\text{A8})$$

As a consequence of the general rule in Eq. (A5), the coefficients sum up to zero. This is a consequence of the rule for derivatives in Eq. (A5). Also note that each operator,  $(\dots \oplus n_i \cdot p_i \oplus \dots)$ , which contributes to  $O_n$  must satisfy the constraint  $\sum n_i p_i = n$ . The expressions in Eq. (A8) give the result of Eq. (8),

$$O_4 = -6(4 \cdot 1) + 12(2 \cdot 1 \oplus 2) - 3(2 \cdot 2) - 4(1 \oplus 3) + (4). \quad (\text{A9})$$

For each  $O_n$  for  $n \geq 2$ , the sum of the coefficients is zero, as can be proved by induction from Eq. (A5).

Using these rules higher order derivatives, needed for the higher order susceptibilities, can be easily written down. Since these manipulations are simple rules for rewriting expressions, not only are they easy to automate inside standard algebra packages, but can even be readily implemented as macros in text editors such as SED or EMACS.

[1] Z. Fodor and S.D. Katz, J. High Energy Phys. **03**, 014 (2002).  
 [2] C.R. Allton *et al.*, Phys. Rev. D **66**, 074507 (2002).  
 [3] M. D’Elia and M.-P. Lombardo, Phys. Rev. D **67**, 014505 (2003).

[4] P. De Forcrand and O. Philipsen, Nucl. Phys. **B642**, 290 (2002).  
 [5] J. Cleymans, J. Phys. G **28**, 1575 (2002).  
 [6] See, for example, U. Heinz, nucl-th/0212004.

- [7] S. Gupta, hep-lat/0301006.
- [8]  $T_c$  stands for the crossover temperature in 2 flavor QCD with finite mass quarks, and the critical temperature in quenched QCD.
- [9]  $Z$  is, of course, real and positive even for  $\mu > 0$ . In the quenched theory valence quarks exist and  $\mu$  acts on them.
- [10] The determinant for each flavor is obtained as usual by taking the fourth root of each staggered quark determinant. As a result, there is a factor of 1/4 for each quark loop evaluated with staggered quarks.
- [11] At vanishing  $\mu$ , the effects of breaking the vector part of the flavor symmetry are small; see R.V. Gavaï and S. Gupta, Phys. Rev. D **66**, 094510 (2002).
- [12] S. Gottlieb *et al.*, Phys. Rev. Lett. **59**, 2247 (1987).
- [13] The derivatives of  $Z$  are called moments, and those of  $\log Z$  are called cumulants, and relations between them can be found in any standard textbook on probability. See, for example, J. G. Kalbfleisch, *Probability and Statistical Inference, Vol. I (Probability)* (Springer-Verlag, New York, 1985).
- [14] S. Gupta, Acta Phys. Pol. B **33**, 4259 (2002).
- [15] R.V. Gavaï, Phys. Rev. D **32**, 519 (1985).
- [16] P. Hasenfratz and F. Karsch, Phys. Lett. **125B**, 308 (1983).
- [17] N. Bilic and R.V. Gavaï, Z. Phys. C **23**, 77 (1984).
- [18] Interestingly, at finite isospin density ( $\mu_u = -\mu_d = \mu_3/2$ ) the expression for  $\Delta P/T^4$  is also given by Eq. (12). For imaginary  $\mu_B$ ,  $\Delta P/T^4$  is negative and the higher order terms in Eq. (12) alternate in sign.
- [19] See, for example, C. Domb and M.S. Green, *Phase Transitions and Critical Phenomena, Vol. III* (Academic, London, 1974).
- [20] S. Gottlieb *et al.*, Phys. Rev. D **35**, 2531 (1987).
- [21] R.V. Gavaï and S. Gupta, Phys. Rev. D **67**, 034501 (2003).
- [22] Our results are stable under change of such algorithmic parameters.
- [23] R.V. Gavaï, S. Gupta, and P. Majumdar, Phys. Rev. D **65**, 054506 (2002).
- [24] A perturbative estimate of  $\chi_{uudd}$  can be obtained from J.-P. Blaizot *et al.*, Phys. Lett. B **523**, 143 (2001), and suggests a value  $O(10^{-3})$ , in excess of the lattice results. Recent estimates from a dimensionally reduced theory agree with them (A. Vuorinen, hep-ph/0305183).
- [25] See also, Z. Fodor *et al.*, hep-lat/0208078.